Open Access

Catalysis Research

LIDSEN Publishing Inc.

Original Research

Effect of ZSM-5 Particle Size and Framework Silica-to-Alumina Ratio on Hexane Aromatization

Manal Al-Eid *, Lianhui Ding, Donya Sewdan, Emad N. AL-Shafei, Rasha Al-Ghamdi, Abdulaziz Alqarawi, Essa Al Naimi

Research and Development Center, Saudi Aramco, Saudi Arabia; E-Mails: manal.eid@aramco.com; lianhui.ding@aramco.com; donya.sewdan@aramco.com; emad.shafei@aramco.com; rasha.ghamdi@aramco.com; abdulaziz.alqarawi@aramco.com; essa.alnaimi@aramco.com

* **Correspondence:** Manal Al-Eid; E-Mail: manal.eid@aramco.com

Academic Editors: Angela Martins and Antonio Chica

Special Issue: Zeolite Materials and Catalysis

Catalysis Research
2022, volume 2, issue 4
doi:10.21926/cr.2204035

Received: August 13, 2022
Accepted: September 19, 2022
Published: October 17, 2022

Abstract

Parent ZSM-5 and Ga-modified ZSM-5 catalysts with different Si/Al ratios and particle sizes were prepared. The physicochemical properties of the prepared catalysts were investigated by performing X-ray powder diffraction analysis, BET surface area analysis, and NH_3-TPD analysis. The performance of the aromatization reaction of the prepared catalysts was evaluated with 1-hexane as a model compound. The zeolite catalysts with a low SiO_2/Al_2O_3 ratio possessed better activity than those with a high SiO_2/Al_2O_3 ratio. Ga modification significantly improved the catalyst aromatization selectivity. Through aromatization, the acid sites of Ga-modified nano-sized zeolites promoted the selective conversion of produced olefin to aromatics by removing H-atoms. For the parent ZSM-5 and Ga-modified catalysts, the catalyst stability increased with an increase in the SiO_2/Al_2O_3 molar ratio. The nano-sized ZSM-5 catalyst with a high SiO_2/Al_2O_3 ratio exhibited better catalytic stability than the microscale ZSM-5, and the nano-sized catalyst with a low SiO_2/Al_2O_3 ratio showed very low stability.

Keywords
Aromatization; n-hexane; H-ZSM-5; Ga-ZSM-5; particle size

1. Introduction

The demand for producing highly valued and marketable products from readily available crude oil products has necessitated the development of high-performance catalysts with better conversion and selectivity [1-3].

Catalytic reforming techniques primarily focus on increasing the efficiency of converting naphthene and paraffins in naphtha feedstock to BTX (benzene, toluene, and xylene) products. The typical feedstock in the reformer is heavy naphtha (boiling range: 65–180 °C). The light naphtha (mainly C5 and C6 alkanes) cannot be converted effectively using conventional reforming catalysts. Several studies have been conducted to develop highly efficient light naphtha aromatization catalysts [4-9]. A study showed that bi-functional catalysts are the most suitable for catalyzing the aromatization of light alkanes [4]. The metal sites on these catalysts are required for dehydrogenation to produce olefin intermediates. These intermediates undergo further cracking and are converted through isomerization or cyclization in the available acid sites of the catalyst to the desirable and more valuable aromatic BTX products [5]. For reforming alkanes and the aromatization process, ZSM-5-based catalysts are the most suitable because of their optimal pore size and three-dimensional interconnected channel system, high acidity, high selectivity, and high activity in many catalytic reforming conversions [6-8]. Balancing the acidity and the metal composition of the ZSM-5 catalysts can increase the catalytic hydro-isomerization of n-alkanes to form BTX products [9]. However, the microporous structure and long diffusion pathway lead to rapid deactivation of the catalysts. These issues decrease selectivity and stability [9].

Since light alkane aromatization reactions are shape-selective, not only does the pore structure and channel system strongly affect the catalyst performance but the channel length and external surface also play an important role. Many studies have investigated the effect of the size of ZSM-5 crystal particles on aromatization performance [10-17]. Smieskova et al. studied the effect of the particle sizes of ion-exchanged Zn/ZSM-5 on the aromatization of light alkanes [10]. Two Zn/ZSM-5 catalysts with ZSM-5 particle sizes <1 μm and about 4 μm were compared during the aromatization of n-hexane. The results indicated that the catalysts with smaller particles enhanced the activity and selectivity compared to those with larger particles. The effect of the particle size of ZSM-5 on hexane cracking was also studied by Mochizuki et al. [11]. They synthesized HZSM-5 with different particle sizes and compared the performance of hexane cracking in the presence of catalysts of different particle sizes, including 1,000 nm, 400 nm, and 100 nm. Irrespective of the size of the particles of the catalyst, the conversion of hexane increased along with an increase in the reaction temperature, and the maximum conversion was recorded at 650 °C. Haag et al. also reported that crystallite size does not affect the cracking of hexane over H-ZSM-5 at 538 °C [12]. These results indicated that the cracking of hexane over H-ZSM-5 is not limited by the diffusion of hexane under the reaction conditions. Slight differences were observed in the behavior of the distribution of the products depending on the crystallite size; the small-sized catalysts showed lower selectivity to propene and butene (1-butnene, 2-butene, and isobutene), whereas the large-sized catalysts showed lower

selectivity to ethylene and BTX (benzene, toluene, and xylenes). When the reaction temperature was increased, the selectivity of the catalyst to propene and butene decreased, while those to ethylene and BTX increased. As the reaction temperature increased, previously formed propene and butene gradually transformed into aromatic compounds, resulting in a decrease in the selectivity of the catalyst to propene and butene products along with an increase in the catalyst selectivity to BTX. The selectivity of the catalyst to ethylene was lower than the selectivity to other alkenes at low temperatures. Ethylene formation occurs via energetically unfavorable primary carbenium ions, irrespective of the unimolecular or bimolecular mechanism. Thus, the apparent activation energy for ethylene formation is high, which is associated with a steep increase in ethylene selectivity with an increase in the reaction temperature. The initial conversion of hexane was almost the same irrespective of the size of the crystallite. The conversion decreased with the reaction time, and the deactivation became faster with an increase in the crystallite size.

The incorporation of gallium into the ZSM-5 zeolite improved the rate-determining dehydration step of olefin during aromatization by reducing the Brønsted acid strength and forming additional stronger Lewis acid sites due to the presence of Ga species, which acted as an extra framework. The catalytic performance of nanosized ZSM-5 zeolites prepared via isomorphous substitution and impregnation of Ga species was investigated for the aromatization of 1-hexane [13]. During aromatization, the nanosized isomorphous Ga-substituted ZSM-5 zeolite samples exhibited higher aromatic yields than the impregnated samples. Yassir et al. [14] investigated the catalytic performance of micro-sized Ga-containing ZSM-5 zeolites. The Ga species were incorporated into the framework of the catalysts using three methods. Compared to micro-sized zeolites, the overall properties of nanocrystalline zeolites, including the mesoporosity features and improved accessibility to internal acid sites, help to overcome the diffusion limitation of the reactants and improve the selectivity to the desired products [15, 16]. Two series of Ga-modified nanosized ZSM-5 were produced by isomorphous substitution and impregnation [17]. To promote highly uniform nucleation, the seed suspension of the nanosized catalysts was prepared using a high-efficiency microwave irradiation heating method. The results of the study indicated that the acid type on the catalysts affected the reaction performance significantly. As the B/L ratio increased, the aromatic yield decreased considerably, indicating that Lewis acid sites favored the conversion of alkanes to aromatics.

The performance of light alkane aromatization catalyst reactions is affected by many closely related factors, such as the catalyst pore structure, acidity, and metal distribution on the support [5-7, 10]. For example, when the Si/Al ratio of the zeolite changed, its acidity and the structure of some pores also changed. Studies on the effect of the particle sizes of zeolites with different Si/Al ratios on light naphtha aromatization are limited. Therefore, in this study, the effect of Si/Al ratio, the diffusion of micro and nano ZSM-5 with different pore length channel structures, and the effect of gallium oxide catalysts on promoting the aromatization of n-hexane as a model compound of light naphtha were examined.

2. Experiments

2.1 Raw Materials

The materials used to prepare ZSM-5 catalysts included the NH_4-formed ZSM-5 zeolites, purchased from Zeolyst, with different SiO_2/Al_2O_3 molar ratios of 25, 30, 50, and 80 ($Na_2O < 0.05$

wt%, surface area > 400 m^2/g, pseudo-boehmite from Sasol (Capapal B, surface area: 250 m^2/g, pore volume: 0.5 mL/g). The aqueous solution of nitric acid and Gallium (III) nitrate hydrate ($Ga(NO_3)_3xH_2O$) were purchased from Fisher Scientific.

2.2 Catalyst Synthesis and Modifications

Five H-form ZSM-5 with different SiO_2/Al_2O_3 ratios (SAR) and particle sizes were used for preparing the catalysts without the addition of metal. The zeolite (80 g) was mixed with the binder made of pseudo-boehmite (20 g, dry-based) peptized with the diluted aqueous solution of nitric acid. The resulting uniform dough was extruded, and the extrudates were dried at 110 °C overnight. The samples were then calcined at 550 °C for 4 h at a heating rate of 2 °C/min. The synthesized micro-sized and nano-sized ZSM-5 were called ZSM-5-m-x and ZSM-5-n-x, respectively, where "m" and "n" represented micro-sized and nano-sized ZSM-5, and "x" represented the SiO_2/Al_2O_3 molar ratio of the zeolite. The catalyst composites and the average particle size (measured by SEM) of the zeolites are summarized in Table 1.

Gallium-containing H-ZSM-5 was prepared by impregnating the above-mentioned ZSM-5 containing catalyst extrudates with an aqueous solution of $Ga(NO_3)_3.xH_2O$. Wet impregnation was performed by adding 10 mL of $Ga(NO_3)_3.xH_2O$ solution containing appropriate quantities of Ga to 8 g of the support of the catalyst. The impregnation was incubated at room temperature for 4 h. Subsequently, the impregnated catalysts were dried in an oven at 110 °C for 24 h and then calcined for 4 h at 550 °C by heating at a rate of 2 °C/min. The details regarding the obtained catalyst samples are also presented in Table 1.

Table 1 A summary of the composition of the catalyst and the average particle size of zeolite.

Catalyst's name	Na_2O, wt.%	Zeolite average particle sizes, nm	Ga, wt.%
ZSM-5-m-30	0.05	4000–5000	--
ZSM-5-m-50	0.05	4000–5000	--
ZSM-5-m-80	0.05	4000–5000	--
ZSM-5-n-25	0.05	<100	--
ZSM-5-n-80	0.05	<100	--
Ga-ZSM-5-m-30	0.05	4000–5000	2.89
Ga-ZSM-5-m-50	0.05	4000–5000	3.36
Ga-ZSM-5-m-80	0.05	4000–5000	2.73
Ga-ZSM-5-n-25	0.05	<100	2.85
Ga-ZSM-5-n-80	0.05	<100	2.83

2.3 Catalyst Characterization

Powder X-ray diffraction (XRD) measurements were performed using the Rigaku Ultima IV multipurpose diffractometer with a copper X-ray tube. The scanning range was set between 2° and 50° in 2θ Bragg-angles with a step size of 0.04°and a total counting time of 1° per minute. The percent crystallinity was calculated using the PANalytical High Score Plus software by comparing it to the crystallinity of a reference sample. The zeolite CBV-28014 purchased from Zeolyst was used

as the reference, and its crystallinity was considered to be 100%. The JCPDS card number used for all zeolites was 01–085–1208.

X-ray fluorescence (XRF) spectroscopy was performed using the Rigaku Ultima IV multipurpose diffractometer to determine the chemical composition of the zeolites. The intensity of the X-rays was processed by the PANalytical WDXRF software (i.e., Omnian) to semi-quantitatively determine the concentrations for the detected elements.

A physisorption analyzer of the Quantachrome Autosorb iQ instrument was used to characterize sample texture properties, including the surface area, pore volume, pore size, and pore size distribution. Before taking measurements, the samples were calcined at 873 K for 4 h. Then, approximately 30–40 mg of the powder samples were degassed in a sample preparation station at 473 K and 1.33×10^{-3} Pa for 15 h. The sample was then switched to the analysis station for adsorption and desorption using liquid nitrogen at 77 K with an equilibrium time of 2 min. The surface area was calculated using the multi-point BET equation with a linear region in the P/Po range of 0.05 to 0.35. The pore volume was calculated from the maximum quantity of nitrogen adsorbed at P/Po = 0.99. The BJH method and the desorption branch of the isotherm were used to determine pore size distribution. The t-plot method was used to identify the microporosity of the product.
The total acidity and the acid strength distribution of the acid zeolites were measured using the Quantachrome Chemstar instrument. Before taking measurements, the sample was pretreated with helium carrier gas at 500 °C for 60 min and cooled down to 50 °C. Then, the sample was exposed to 10% NH_3 in He for 30 min. To remove the physiosorbed ammonia, the sample was followed by purging with helium gas at 50 °C for 60 min. The ammonia temperature-programmed desorption (NH_3-TPD) test was then conducted from 50 to 700 °C at a heating rate of 10 °C/min.

2.4 Evaluating the Performance of Catalytic Reactions

The performance of aromatization reactions in the presence of ZSM-5 zeolite-containing catalysts was evaluated in a 16-fold high-throughput fixed-bed reactor system. In each reactor, 1.5 g of catalyst extrudates (OD 1.5 mm, L = 2–4 mm) were loaded. The catalysts were pretreated with H_2 at 200 °C for 4 h and 500 °C for 10 h. After pretreatment, hydrogen was replaced by nitrogen, and the temperature was increased to 550 °C. Then, liquid hexane was added, and the reaction was performed at a temperature of 550 °C, the total pressure of 1 bar, weight hourly space velocity (WHSV) of 12 h^{-1}, and a nitrogen/n-hexane volume ratio of 200:1. All products were analyzed by performing online gas chromatography (GC).

3. Results and Discussion

3.1 X-ray Diffraction (XRD) Characterization

The XRD powder patterns and the relative crystallinity of H-ZSM-5 and Ga/H-ZSM-5 catalysts with different SiO_2/Al_2O_3 ratios and different particle sizes are shown in Figure 1. The patterns exhibited the characteristic peaks in the 7–9° and 22–25° region of 2θ, attributed to the diffraction of the respective crystalline planes of the MFI framework. Due to the addition of 20% alumina (as a binder), the crystallinity of the zeolite in the catalyst could be calculated by dividing the XRD-measured crystallinity of the catalyst by 80%. The actual crystallinity of the zeolites is summarized in Table 2.

The results showed that the crystallinity of all zeolites was well-maintained after adding 20 wt.% of the binder.

After adding Ga to the ZSM-5 zeolite, the characteristic peaks of the Ga species were not observed, which indicated that the Ga species were well-distributed on ZSM-5 zeolite and alumina. The change in the crystallinity of the catalysts before and after the addition of Ga is shown in Figure 2. After adding Ga, the crystallinity of Ga-containing catalysts decreased by 2–17%, indicating that the Ga species damaged some zeolite structures. The crystallinity of the nano-sized zeolite catalysts was lower than that of the micro-sized zeolite catalysts, especially for ZSM-5-n-25. Further studies need to be conducted to determine ways to maintain the crystallinity of nano-sized ZSM-5 after adding Ga. For example, after selecting appropriate Ga compounds, suitable metal-loading and special activation procedures need to be conducted before testing the catalyst.

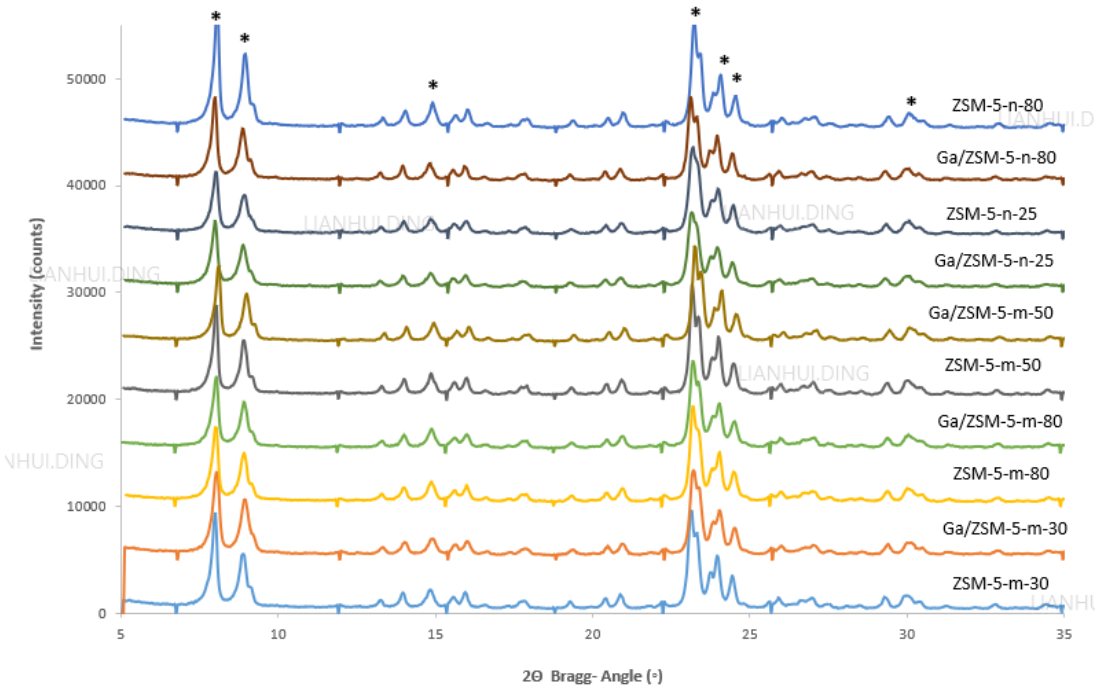

Figure 1 The XRD patterns of parent and metal-modified ZSM-5 catalysts; '*' indicates ZSM-5 characteristic peaks.

Table 2 The crystallinity and the elemental composition of the parent and Ga/H-ZSM-5 catalysts.

Sample name	Relative Crystallinity (%)	
	For the catalyst	For the zeolite in the catalyst
ZSM-5-m-30	80.4	100.5
ZSM-5-m-50	79.7	99.6
ZSM-5-m-80	80.5	100.6
ZSM-5-n-25	78.0	97.5
ZSM-5-n-80	81.0	101.3
Ga-ZSM-5-m-30	72.3	90.4
Ga-ZSM-5-m-50	78.0	97.5

Ga-ZSM-5-m-80	74.3	92.9
Ga-ZSM-5-n-25	66.4	83.0
Ga-ZSM-5-n-80	71.7	89.6

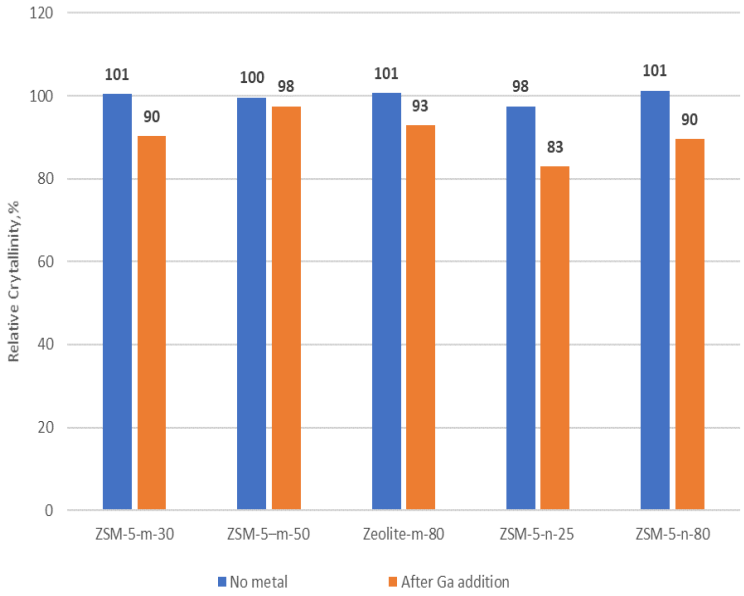

Figure 2 Changes in the crystallinity of the catalysts before and after the addition of Ga.

3.2 Catalyst Textural Properties

The textural properties based on nitrogen adsorption are shown in Figure 3 and Table 3. All samples exhibited typical type-IV curves with an increase at the relative pressure (P/P_0) of 0.40–0.90 due to capillary condensation in the mesopores.

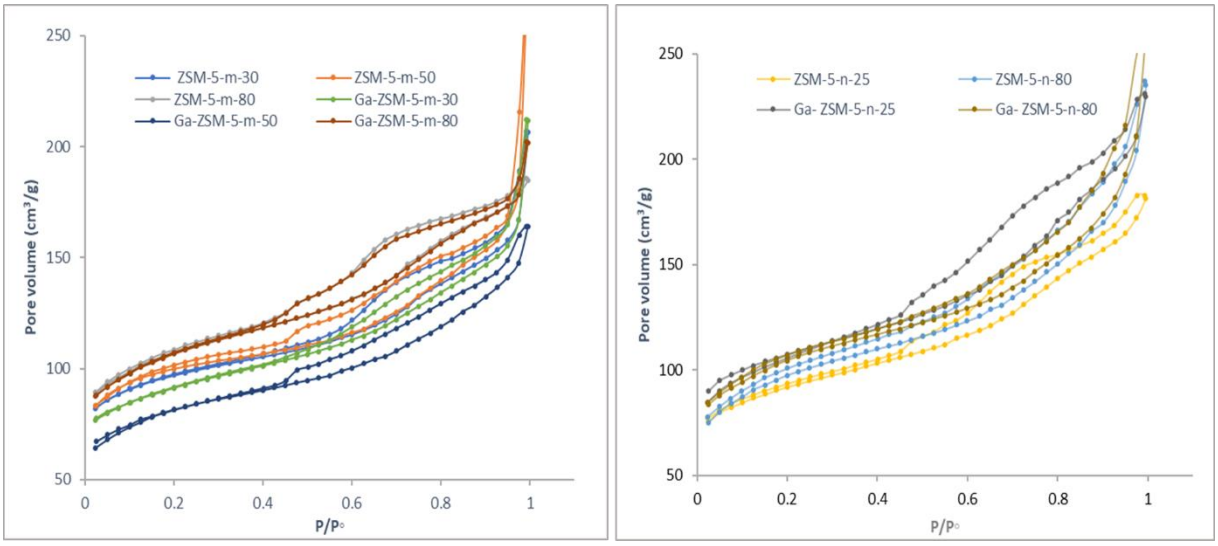

Figure 3 The nitrogen adsorption–desorption isotherms of parent and metal-modified ZSM-5 catalysts.

Table 3 The BET surface areas and pore volumes of parent and metal-modified ZSM-5 catalysts.

Sample	[a] S_{Total} ($m^2 g^{-1}$)	[b] S_{mes} ($m^2 g^{-1}$)	[c] S_{micro} ($m^2 g^{-1}$)	[d] V_{total} ($cm^3 g^{-1}$)	[e] V_{mes} ($cm^3 g^{-1}$)	[g] V_{mic} ($cm^3 g^{-1}$)	Average pore size(Å)
ZSM-5-m-30	308	140	168	0.32	0.23	0.09	42
ZSM-5-m-50	274	138	136	0.27	0.2	0.07	39
ZSM-5-m-80	349	182	167	0.28	0.19	0.09	32
ZSM-5-n-25	297	161	136	0.28	0.21	0.07	38
ZSM-5-n-80	321	218	103	0.36	0.31	0.05	45
Ga-ZSM-5-m-30	293	143	150	0.33	0.25	0.08	45
Ga-ZSM-5-m-50	264	118	146	0.25	0.19	0.06	38
Ga-ZSM-5-m-80	349	189	160	0.31	0.23	0.08	36
Ga-ZSM-5-n-25	349	143	111	0.35	0.19	0.06	40
Ga-ZSM-5-n-80	341	170	171	0.39	0.3	0.09	46

[a] S_{BET} is the BET surface area obtained from N_2 adsorption; [b] S_{meso} is the mesoporous surface area evaluated from t-plot method; [c] S_{microt} is the microporous surface area; [d] V_{tot} is the total pore volume; [e] V_{mes} is the Mesoporous volume; [f] V_{mes} (%) is the percentage of mesopore volume; [g] V_{mic} is the microspore volume.

In the absence of Ga, for micro-sized zeolite-containing catalysts, the SiO_2/Al_2O_3 ratio increased, the total surface area and average pore size increased, and the total pore volume slightly decreased; for nano-sized zeolite-containing catalysts, the total surface area, pore volume, and average pore size increased considerably. More mesopores were formed probably due to interparticle spaces [18].

After adding Ga for all catalysts, the textual properties were almost unchanged, indicating that the Ga species were well-dispersed on the zeolites. These results were similar to those of the XRD analysis.

The BJH pore-size distribution curves for all catalysts are shown in Figure 4, which shows the presence of mesopore systems in the synthesized products. The results of pore size distribution showed that the mesopore size was around 1.7 nm in all ZSM-5 samples. However, the distribution of these mesopores decreased considerably after the samples underwent Ga treatment.

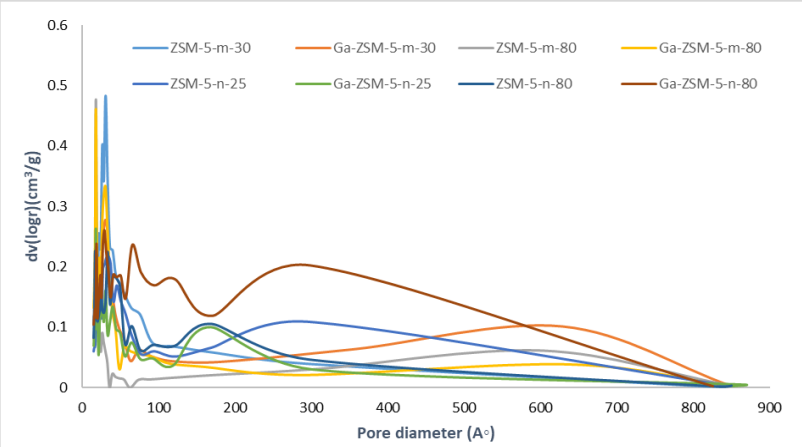

Figure 4 The BJH pore size distribution of parent and metal-modified ZSM-5 catalysts.

3.3 Catalyst Acidity Properties

The acidity of the ZSM-5 catalysts and the Ga/ZSM-5 catalysts was characterized by NH_3-TPD. The results are shown in Figure 5 and Table 4. Weak or strong acidity was arbitrarily defined as acidic sites corresponding to the quantity of desorbed NH_3 at <300 °C or >300 °C, respectively.

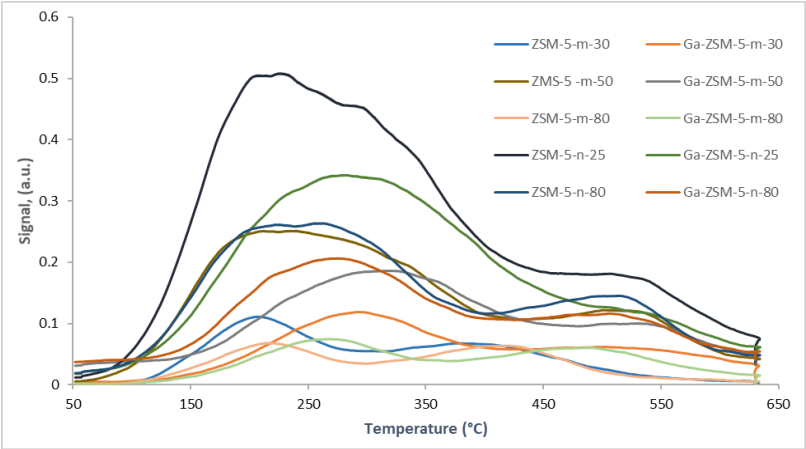

Figure 5 The NH_3-TPD profiles for parent and metal-modified ZSM-5 zeolite catalysts.

Table 4 The Acid Site Distribution of parent and metal-modified ZSM-5 catalysts.

Sample name	Total Acidity (mmol/g)	Week acidity Ratio < 300 °C (%)	Strong Acidity Ratio > 300 °C (%)	Max Peak Temperature, (°C)	
				Low	High
ZSM-5-m-30	1.1	63.0	37.0	212	430
ZSM-5-m-50	3.0	56.0	44.0	261	544
ZSM-5-m-80	0.8	52.8	47.2	207	435
ZSM-5-n-25	5.0	60.1	39.9	239	537
ZSM-5-n-80	2.9	54.2	45.8	265	507
Ga-ZSM-5-m-30	0.9	47.8	52.2	298	544
Ga-ZSM-5-m-50	1.6	42.9	57.1	326	546
Ga-ZSM-5-m-80	0.8	45.4	54.6	280	502
Ga-ZSM-5-n-25	3.5	53.4	46.6	287	547
Ga-ZSM-5-n-80	1.7	46.3	53.7	266	527

For the zeolite catalysts with a similar SiO_2/Al_2O_3 molar ratio, when the particle sizes decreased from the micrometer to the nanometer scale, the acidity increased significantly. This finding confirmed the results of previous studies, which showed that the acidity of nano-sized ZSM-5 was comparable to or higher than that of micro-sized ZSM-5 [19-21]. Compared to the acidity of ZSM-5-m-30 and ZSM-5-m-80, the acidity of ZSM-5-n-25 and ZSM-5-n-80 increased by 4.5 and 3.6 times, respectively. After particle size reduction, the acidity distribution changed slightly: (1) strong acidity increased slightly (by about 2%); (2) the peak temperature corresponding to weak and strong acidity shifted to a higher temperature, which indicated that after particle size reduction, not only did the acidic concentration of the catalysts increase but the strength of acidity also increased. In our study,

the ZSM-5 zeolite was mixed with the binder to form the extrudates. Compared to the micro-sized zeolites, less acidic sites in the zeolite channels were lost due to pore blockage, and more acidic sites were located on external surfaces that could be easily accessed by the probe NH_3 molecules. Therefore, nano-sized ZSM-5-containing catalysts showed higher acidity.

After loading Ga oxide, compared to the acidity of their corresponding support catalysts, the acidity of all catalysts decreased, and the ratio of strong acidity increased substantially. The Ga oxide species interacted with some acidic sites and covered them. From the acidity distribution, we found that weaker acid sites were affected by the addition of Ga oxide. Except for the catalyst with the zeolite SiO_2/Al_2O_3 molar ratio of 80, the acidity decreased by 50–80%, irrespective of the zeolite SiO_2/Al_2O_3 molar ratio. Several studies [13, 22-24] on Ga impregnation found that after impregnated catalyst calcination, the Ga_2O_3 phase and small amounts of GaO species are formed and located mainly on the external surface of the zeolites. These Ga species, especially the GaO species, can cover some acidic sites and decrease the total acidity.

3.4 Aromatization Reaction Performance of n-hexane

3.4.1 Effect of the Si/Al Ratio and Particle Size on the Conversion of Hexane

The conversion of hexane by all catalysts is summarized in Table 5. Similar to the findings of previous studies [22], we found that the activity of ZSM-5-containing catalysts decreased during hexane aromatization with an increase in the SiO_2/Al_2O_3 ratio of the zeolites due to a decrease in total acidity. When the zeolites had a SiO_2/Al_2O_3 ratio of 25–30, the conversion of hexane was similar (99.6 wt.%) for the micro-sized and nano-sized zeolite-containing catalysts. However, when the SiO_2/Al_2O_3 ratio increased from 30 to 80, for micro-sized zeolite-containing catalysts, the conversion decreased from 99.6 wt.% to 88.0 wt.%, while for nano-sized zeolite-containing catalysts, the conversion decreased from 99.6 wt% only to 99.2 wt.%. The main reason for the difference was that the nano-sized zeolite catalysts were more acidic. Even when the SiO_2/Al_2O_3 ratio increased to 80, the acidity (2.9 mmol/g) of the nano-sized zeolite catalyst was considerably higher than that (1.1 mmol/g) of the micro-sized catalyst with a SiO_2/Al_2O_3 ratio of 30.

Table 5 Hexane conversion and product yield of parent ZSM-5 and Ga-modified ZSM-5 catalysts.

Catalyst	Conversion, %	n-Hexane %	H_2 %	Paraffin %	Olefin %	Naph* %	Arm** %
ZSM-5-m-30	99.57	0.41	1.28	54.71	7.63	0.06	36.32
ZSM-5-m-50	99.73	0.27	0.91	61.02	5.39	0.08	32.58
ZSM-5-m-80	88.04	11.97	0.59	63.87	17.26	0.43	17.85
ZSM-5-n-25	99.63	0.36	1.38	54.75	5.00	0.05	38.82
ZSM-5-n-80	99.20	0.80	0.74	62.44	10.74	0.19	25.88
Ga-ZSM-5-m-30	98.41	1.50	3.17	39.22	6.82	0.06	50.77
Ga-ZSM-5-m-50	93.66	5.95	2.96	41.52	10.27	0.12	45.16
Ga-ZSM-5-m-80	83.20	16.20	2.30	48.94	14.65	0.21	33.92

Ga-ZSM-5-n-25	98.37	1.55	3.26	38.26	6.70	0.05	51.75
Ga-ZSM-5-n-80	96.50	3.30	2.91	41.48	10.26	0.12	45.27

Operation conditions: 550 °C, WHSV of 12 h −1, 1 bar pressure, TOS of 48 h. * Naph: naphthene, ** Arm: Aromatics.

After loading Ga, for all catalysts, the conversion of hexane decreased slightly, probably due to the covering of some acid sites. A slight decrease in the conversion by nano-sized zeolite catalysts might be caused due to a greater loss of zeolite crystallinity channeling than that in the micro-sized zeolite catalysts. The effect of zeolite crystallinity on n-hexane aromatization using Ga, Zn, and Mo-modified catalysts was previously studied [24]. The results indicated that with an increase in zeolite crystallinity, the conversion and the yield of aromatics via n-hexane aromatization increased. Therefore, better methods need to be developed to preserve zeolite crystallinity during the synthesis and modification of zeolite and the catalyst. Further studies need to be conducted to determine ways to maintain the crystallinity of nano-sized zeolite, which in turn can further improve the reaction performance compared to the performance of micro-sized zeolite-containing catalysts.

3.4.2 Effect of the Si/Al Ratio and Particle Size on Product Selectivity

The main products formed by hexane aromatization included aromatics, hydrogen, a mixture of n-paraffins and iso-paraffins (mainly C1-C4, iso-paraffin < 10%), naphthene, and olefins. The yield of the main products of hexane aromatization reactions is summarized in Table 4. The effect of the SiO_2/Al_2O_3 molar ratio on the yield of the micro-sized zeolite-containing catalysts without and with the addition of Ga is shown in Figure 6 and Figure 7, respectively. In both figures, “N” represents “naphthene”, and “A” represents “aromatics”. Aromatics, hydrogen, and olefins are highly valuable and expected products. For all catalysts, when the SiO_2/Al_2O_3 molar ratio increased from 30 to 80, the yield of H_2 and aromatics decreased considerably, while the yield of olefin increased for all catalysts, and negligible amounts of naphthene were produced. However, the nano-sized zeolite catalysts had substantially higher hydrogen and aromatics yields and lower olefin yields than micro-sized zeolite catalysts. The acidic sites of the zeolites were mainly contributed by the negatively-charged tetrahedral aluminum. As the aluminum content in the zeolite framework increased, the acidic sites increased, and acidity decreased. As the main reactions in the aromatization of light alkanes, cracking, hydrogen transfer, and cyclization occurred at the acid sites of the catalysts. The presence of more acid sites and lower acidity of low SAR zeolites led to higher activity and a decrease in the cracking of the intermediates, resulting in greater aromatic yield.

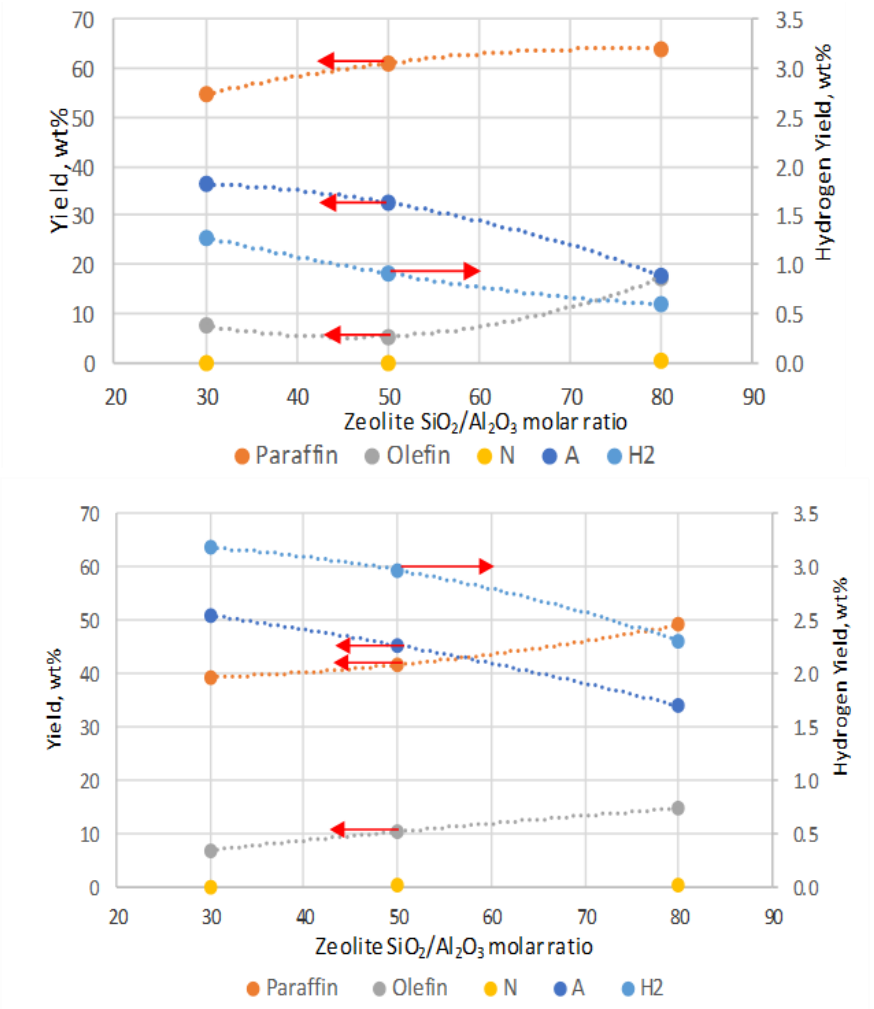

Figure 6 The product yield with micro-sized parent ZSM-5 catalysts (A) and Ga-modified ZSM-5 catalysts (B).

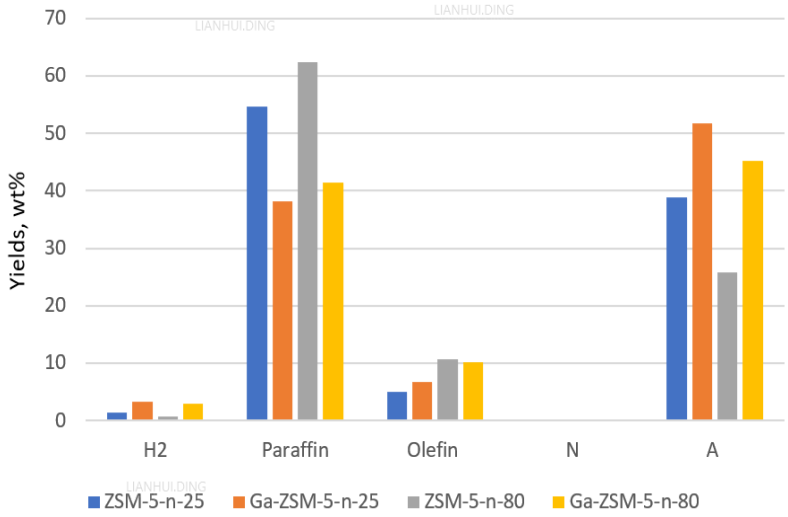

Figure 7 The product yield with nano-sized zeolite catalysts.

For the same amount of zeolites added to the catalysts, the zeolites with small particles (especially in the nano-size range) provided more accessible acidic sites, especially those located on

the external surface. For Ga-modified catalysts, more nano-sized zeolites were distributed in the adjacent areas of the Ga species. Higher acidic sites and better "contact" with Ga favored the cyclization and aromatization of the intermediate olefin. Hence, the nano-sized zeolite-containing catalysts yielded more aromatics and hydrogen than the micro-sized zeolite-containing catalysts.

Some studies found that the aromatization [25, 26] of light alkanes could be categorized into two main reaction mechanisms, including the bifunctional reaction mechanism (e.g., ZSM-5-based catalysts) and the monofunctional mechanism (e.g., KL-based catalysts). Many researchers have found that the aromatization of light alkanes occurs in three stages, which include the formation of alkenes from the starting alkane, the interconversion of olefins, and the transformation of olefins into aromatic compounds [25, 26]. The simplified scheme of hexane aromatization is illustrated in Scheme 1. The first step is the transformation of an alkane, which occurs in two ways, i.e., cracking and hydrogen transfer (dehydrogenation). In the method involving hydrogen transfer, the reaction occurs between the alkane and the product alkane adsorbed on the acid sites of the zeolites. The interconversion step includes the isomerization of alkenes and oligomerization, followed by cracking. In the third step, the aromatization of alkenes occurs by ZSM-5. During the interconversion of alkene, the aromatization proceeds via cyclization and dehydrogenation reactions. As shown in the scheme, hydrogen is produced via naphthene dehydrogenation or the direct cyclization of olefin. Only a small amount of hydrogen is consumed during the conversion of olefin to paraffins. Therefore, hydrogen yield either decreases or increases with the yield of aromatics. Only trace amounts of naphthene were detected in the products either because most aromatics were generated by the direct cyclization of olefins or because the naphthene intermediate was quickly converted to aromatics.

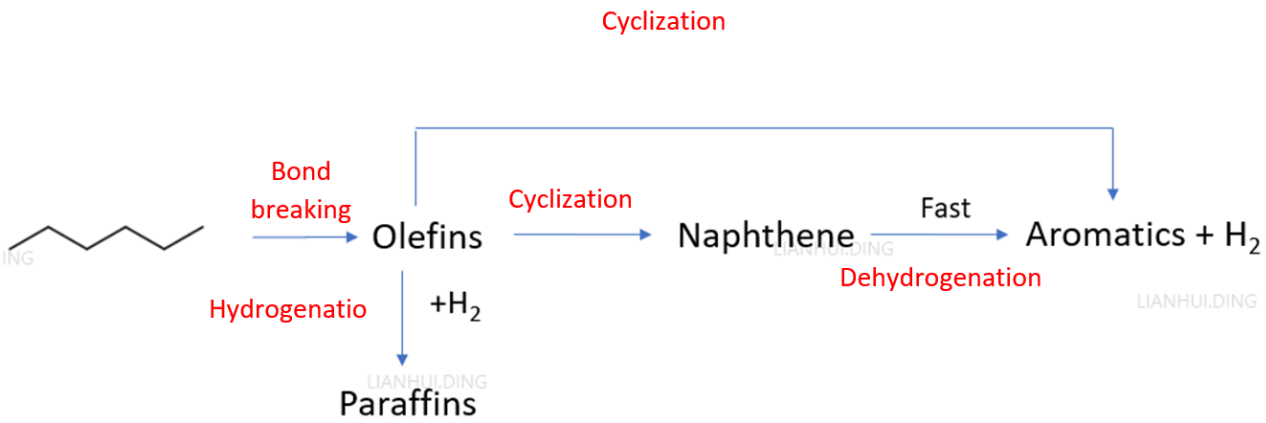

Scheme 1 Hexane aromatization.

After the addition of Ga, aromatization was enhanced for all catalysts. The nano-sized zeolite catalysts showed a better reaction performance than the micro-sized zeolite catalysts, although the nano-sized zeolites had lower crystallinity caused by the addition of Ga. If the crystallinity of nano-sized zeolite can be retained or improved after adding Ga, its reaction performance can be further improved. Studies [27-35] have found that Ga can promote the selective conversion of the olefin produced to aromatics by removing H-atoms via the acid sites that activate C-H bonds. This allows the acid sites to turnover without the formation of cracking products. Ga and Zn act as portholes and catalyze the re-combinative desorption of H-atoms formed during the acid-catalyzed C-H bond

cleavage to H_2. The removal of H_2 reduces the formation of unwanted by-products, such as methane and ethane.

3.4.3 Effect of Particle Size on Catalyst Stability

To evaluate the stability of the catalysts, the hexane conversion changes with time (time on stream: 45 h) were compared. The results for parent ZSM-5-based catalysts and Ga-modified zeolite catalysts are illustrated in Figure 8 and Figure 9, respectively.

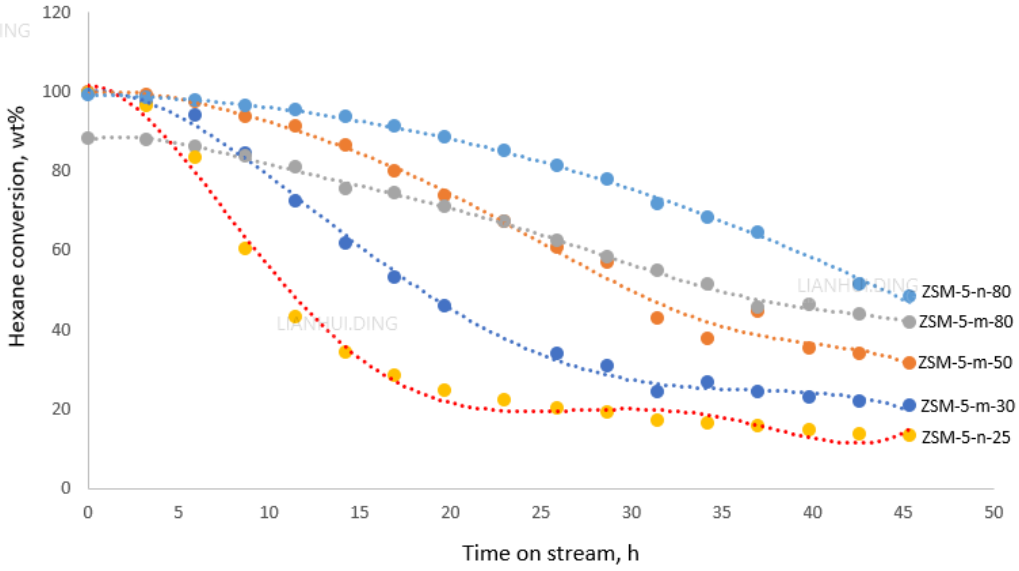

Figure 8 The stability of the parent ZSM-5 catalysts.

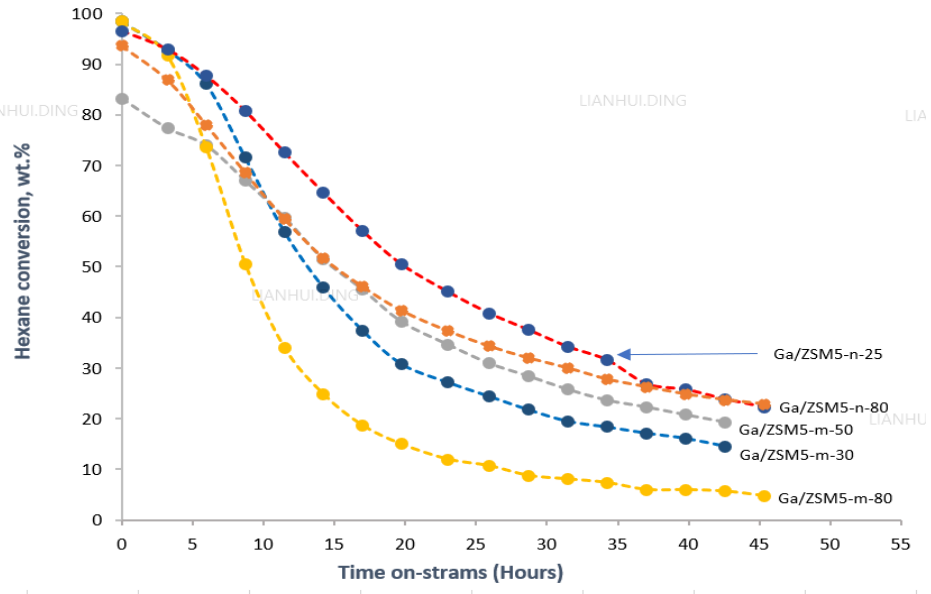

Figure 9 The stability of Ga-modified ZSM-5 catalysts.

For parent micro-sized ZSM-5 catalysts, as the SiO_2/Al_2O_3 molar ratio increased, the catalyst stability also increased. When the ZSM-5 particle size decreased to nano-size, very low stability was observed for the ZSM-5 catalyst with a low SiO_2/Al_2O_3 ratio. However, the nano-sized ZSM-5 catalyst

with a high SiO_2/Al_2O_3 ratio showed the highest stability. After Ga modification, a similar trend was observed. Coking is the main reason for catalyst deactivation. Some studies [26] have shown that adding Ga has a positive effect on the conversion of *n*-hexane for the catalysts with lower gallium loadings. With a further increase in Ga loading, the deactivation of the catalyst can become more severe. Similar results were also reported for catalysts with high Ga loadings by Lanh et al. [33]. It was attributed to an increase in the amount of non-framework gallium species, which are responsible for strong deactivation due to an increase in the formation of olefinic compounds that are regarded as coke precursors.

The decrease in the Al content of the zeolite was not sufficient to ensure a low rate of coke formation. The zeolite pore structure strongly influences the resistance of coking [36-39]. For example, the unique pore structure of ZSM-12 consisting of one-dimensional channels of constant diameter along with reduced acidity increases its stability. Although L zeolite possesses one-dimensional channels, it deactivates rapidly. This might be because the channel openings of L zeolite vary periodically along the direction of pores from 7.5 Å to 13 Å [34, 35]. This configuration of pores allows the buildup of coke, probably in the "enlargements" of zeolite channels. The stability of a catalyst is related to acidity and pore structure. To achieve better acidity and catalysts with higher stability, the acidity and pore structure need to be well-balanced and tuned. Finally, the study emphasized the importance of Ga and ZSM-5 with a low SiO_2/Al_2O_3 ratio to promote the aromatization of hexane. Further studies on stabilized frameworks of zeolite need to be conducted to develop better zeolite catalysts.

4. Conclusion

The nano-sized zeolite catalysts with a lower SiO_2/Al_2O_3 ratio were more vulnerable than those with a higher SiO_2/Al_2O_3 ratio to the destruction of the structure due to the addition of Ga. The results of the XRD and BET analyses indicated that the Ga species were well-dispersed on the zeolites. When the particle sizes decreased from the micrometer to the nanometer scale, the acidity increased significantly. After loading Ga, the acidity decreased for all catalysts compared to the acidity of their corresponding support catalysts, and the ratio of strong acidity greatly increased; weak acid sites were affected more by the addition of Ga.

The activity of the ZSM-5-containing catalyst related to hexane aromatization decreased with an increase in the SiO_2/Al_2O_3 ratio of the zeolites due to the decrease in total acidity. For both micro-sized and nano-sized zeolite-containing catalysts with a SiO_2/Al_2O_3 ratio of 25–30, the initial activity was similar. However, when the SiO_2/Al_2O_3 ratio increased to 80, hexane conversion by the micro-sized zeolite-containing catalyst decreased considerably, while for the nano-sized zeolite-containing catalyst, the conversion was well-maintained. After Ga loading, for all catalysts, probably due to the covering of some acid sites, the conversion of hexane decreased slightly. For all catalysts, when the SiO_2/Al_2O_3 molar ratio increased from 30 to 80, the yield of H_2 and aromatics decreased substantially, while the olefin yield increased, and a negligible amount of naphthene was produced. The nano-sized zeolite catalysts had a considerably higher yield of hydrogen and aromatics than the micro-sized zeolite catalysts but considerably lower olefin yield. For the parent ZSM-5 catalysts and Ga-modified catalysts, as the SiO_2/Al_2O_3 molar ratio increased, the stability of the catalyst also increased. When the ZSM-5 particle size was reduced to nano-size, very low stability was observed for the ZSM-

5 catalyst with a low SiO_2/Al_2O_3 ratio. However, the nano-sized ZSM-5 catalyst with a high SiO_2/Al_2O_3 ratio had very high stability because the pores were small.

Acknowledgments

The authors would like to thank Hassan Sadiq & Ali Al-Nasser for the support in catalyst characterization.

Author Contributions

Manal Eid: project development, catalyst synthesis and characterization, experiment design and data processing. Lianhui Ding: project development, experiment and catalyst synthesis design, catalyst performance evaluation, and data processing. Donya Sewdan: Catalyst synthesis and characterization. Emad N. AL-Shafei: catalyst testing and date processing. Rasha Al-Ghamdi: Catalyst characterization. Abdulaziz Alqarawi: catalyst testing and data processing. Essa Al Naimi: project lead, project development, catalyst synthesis and testing design, and data processing.

Competing Interests

The authors have declared that no competing interests exist.

References

1. Corma A, Martinez A. Catalysis on porous solids. In: Handbook of porous solids. Weinheim: WILEY-VCH; 2002. pp. 2825-2922.
2. Farrauto RJ, Bartholomew CH. Fundamentals of industrial catalytic processes. London: Academic and Professional; 1997.
3. Vermeiren W, Gilson JP. Impact of zeolites on the petroleum and petrochemical industry. Top Catal. 2009; 52: 1131-1161.
4. Lugstein A, Jentys A, Vinek H. Hydroisomerization and cracking of n-octane and C_8 isomers on Ni-containing zeolites. Appl Catal A. 1999; 176: 119-128.
5. Lugstein A, Jentys A, Vinek H. Hydroconversion of n-heptane over bifunctional HZSM5 zeolites influence of the metal concentration and distribution on the activity and selectivity. Appl Catal A. 1998; 166: 29-38.
6. Xu Y, Lin L. Recent advances in methane dehydro-aromatization over transition metal ion-modified zeolite catalysts under non-oxidative conditions. Appl Catal A. 1999; 188: 53-67.
7. Pereira MS, da Silva AM, Nascimento MAC. Effect of the zeolite cavity on the mechanism of dehydrogenation of light alkanes over gallium-containing zeolites. J Phys Chem C. 2011; 115: 10104-10113.
8. Song C, Liu K, Zhang D, Liu S, Li X, Xie S, et al. Effect of cofeeding n-butane with methanol on aromatization performance and coke formation over a Zn loaded ZSM-5/ZSM-11 zeolite. Appl Catal A. 2014; 470: 15-23.
9. Ji Y, Yang H, Yan W. Strategies to enhance the catalytic performance of ZSM-5 zeolite in hydrocarbon cracking: A review. Catalysts. 2017; 7: 367.
10. Smiešková A, Rojasová E, Hudec P, Šabo L. Aromatization of light alkanes over ZSM-5 catalysts: Influence of the particle properties of the zeolite. Appl Catal A. 2004; 268: 235-240.

11. Mochizuki H, Yokoi T, Imai H, Watanabe R, Namba S, Kondo JN, et al. Facile control of crystallite size of ZSM-5 catalyst for cracking of hexane. Microporous Mesoporous Mater. 2011; 145: 165-171.
12. Haag WO, Lago RM, Weisz PB. Transport and reactivity of hydrocarbon molecules in a shape-selective zeolite. Faraday Discuss Chem Soc. 1981; 72: 317-330.
13. Fang Y, Su X, Bai X, Wu W, Wang G, Xiao L, et al. Aromatization over nanosized Ga-containing ZSM-5 zeolites prepared by different methods: Effect of acidity of active Ga species on the catalytic performance. J Energy Chem. 2017; 26: 768-775.
14. Al-Yassir N, Akhtar MN, Al-Khattaf S. Physicochemical properties and catalytic performance of galloaluminosilicate in aromatization of lower alkanes: A comparative study with Ga/HZSM-5. J Porous Mater. 2012; 19: 943-960.
15. Fu T, Chang J, Shao J, Li Z. Fabrication of a nano-sized ZSM-5 zeolite with intercrystalline mesopores for conversion of methanol to gasoline. J Energy Chem. 2017; 26: 139-146.
16. Tago T, Konno H, Sakamoto M, Nakasaka Y, Masuda T. Selective synthesis for light olefins from acetone over ZSM-5 zeolites with nano- and macro-crystal sizes. Appl Catal A. 2011; 403: 183-191.
17. Su X, Wang G, Bai X, Wu W, Xiao L, Fang Y, et al. Synthesis of nanosized HZSM-5 zeolites isomorphously substituted by gallium and their catalytic performance in the aromatization. Chem Eng J. 2016; 293: 365-375.
18. Yang L, Liu Z, Liu Z, Peng W, Liu Y, Liu C. Correlation between H-ZSM-5 crystal size and catalytic performance in the methanol-to-aromatics reaction. Chinese J Catal. 2017; 38: 683-690.
19. Viswanadham N, Saxena SK, Kumar J, Sreenivasulu P, Nandan D. Catalytic performance of nano crystalline H-ZSM-5 in ethanol to gasoline (ETG) reaction. Fuel. 2012; 95: 298-304.
20. Viswanadham N, Saxena SK. Enhanced performance of nano-crystalline ZSM-5 in acetone to gasoline (ATG) reaction. Fuel. 2013; 105: 490-495.
21. Camblor MA, Corma A, Valencia S. Characterization of nanocrystalline zeolite Beta. Microporous Mesoporous Mater. 1998; 25: 59-74.
22. Ausavasukhi A, Sooknoi T. Tunable activity of [Ga]HZSM-5 with H_2 treatment: Ethane dehydrogenation. Catal Commun. 2014; 45: 63-68.
23. Xiao H, Zhang J, Wang X, Zhang Q, Xie H, Han Y, et al. A highly efficient Ga/ZSM-5 catalyst prepared by formic acid impregnation and in situ treatment for propane aromatization. Catal Sci Technol. 2015; 5: 4081-4090.
24. Xiao H, Zhang J, Wang P, Zhang Z, Zhang Q, Xie H, et al. Mechanistic insight to acidity effects of Ga/HZSM-5 on its activity for propane aromatization. RSC Adv. 2015; 5: 92222-92233.
25. Fung J, Wang I, The Reaction Mechanism of C6 Hydrocarbons over Acid–Base Bifunctional Catalysts, TiO2–ZrO2, J. of Catal. 1996; 164; 166-172.
26. Guisnet M, Gnep NS. Mechanism of short-chain alkane transformation over protonic zeolites. Alkylation, disproportionation and aromatization. Appl Catal A-Gen. 1996; 146: 33-64.
27. Janardhan HL. Studies on modified zeolite catalysts for aromatization and aromatic substitution reactions. Karnataka: Manipal University; 2015.
28. Tshabalala TE. Aromatization of n-hexane over metal modified H-ZSM-5 zeolite catalysts. Johannesburg: University of the Witwatersrand; 2009.
29. Guisnet M, Gnep N. Mechanism of short-chain alkane transformation over protonic zeolites. Alkylation, disproportionation and aromatization. Appl Catal A. 1996; 146: 33-64.

30. Nguyen LH, Vazhnova T, Kolaczkowski ST, Lukyanov DB. Combined experimental and kinetic modelling studies of the pathways of propane and n-butane aromatization over H-ZSM-5 catalyst. Chem Eng Sci. 2006; 61: 5881-5894.
31. Kohler MA, Wainwright MS, Trimm DL, Cant NW. Reaction kinetics and selectivity of dimethyl succinate hydrogenolysis over copper-based catalysts. Ind Eng Chem Res. 1987; 26: 652-656.
32. Nakamura I, Fujimoto K. On the role of gallium for the aromatization of lower paraffins with Ga-promoted ZSM-5 catalysts. Catal Today. 1996; 31: 335-344.
33. Biscardi JA, Iglesia E. Structure and function of metal cations in light alkane reactions catalyzed by modified H-ZSM5. Catal Today. 1996; 31: 207-231.
34. Choudhary VR, Mulla SAR, Banerjee S. Aromatization of n-heptane over H-AlMFI, Ga/H-AlMFI, H-GaMFI and H-GaAlMFI zeolite catalysts: Influence of zeolitic acidity and non-framework gallium. Microporous Mesoporous Mater. 2003; 57: 317-322.
35. Lanh HD, Tuan VA, Kosslick H, Parlitz B, Fricke R, Völter J. N-Hexane aromatization on synthetic gallosilicates with MFI structure. Appl Catal A. 1993; 103: 205-222.
36. Smirniotis PG, Zhang W. Effect of the Si/Al ratio and of the zeolite structure on the performance of dealuminated zeolites for the reforming of hydrocarbon mixtures. Ind Eng Chem Res. 1996; 35: 3055-3066.
37. Newsam J. Structures of dehydrated potassium zeolite L at 298 and 78 K and at 78 K containing sorbed perdeuteriobenzene. J Phys Chem. 1989; 93: 7689-7694.
38. Le Van Mao R, Dufresne LA, Yao J, Yu Y. Effect of the nature of coke on the activity and stability of the hybrid catalyst used in the aromatization of ethylene and n-butane. Appl Catal A. 1997; 164: 81-89.
39. Viswanadham N, Dhar GM, Rao TP. Pore size analysis of ZSM-5 catalysts in n-heptane aromatization reaction: An evidence for molecular traffic control (MTC) mechanism. J Mol Catal A. 1997; 125: L87-L90.